Desalination and Water Treatment
www.deswater.com

doi: 10.5004/dwt.2021.27059

221 (2021) 76–84
May

Optimization of chloride ion removal from desulfurization wastewater by electrocatalysis progress: application of Box–Behnken design

Jianghua Peng[a,b], Houzhang Tan[a,*], Ping Yu[c]

[a]*MOE Key Laboratory of Thermo-Fluid Science and Engineering, School of Energy and Power Engineering, Xi'an Jiaotong University, No. 28 Xianning West Road, Xi'an, Shaanxi 710049, China, Tel. +086-029-82668051; Fax: +86-029-82668703; email: hzt@mail.xjtu.edu.cn*
[b]*Xinjiang Energy Co., Ltd., Urumchi 830000, China*
[c]*College of Chemistry and Molecular Sciences, Wuhan University, Wuhan 430072, China*

Received 22 May 2020; Accepted 31 December 2020

ABSTRACT

At present, it is difficult to remove the ultra-high concentration of chloride ions (about 20,000 mg/L) in desulfurization wastewater by traditional methods. The aim of this work was to evaluate the removal of chloride ions from desulfurization wastewater by electro-catalysis progress using $Ti/SnO_2–Sb_2O_3/PbO_2$ electrodes. Response surface methodology (Box–Behnken design (BBD)) was employed to investigate the effects of current density, pH value, and electrolysis time on the removal of chloride ions. Three factors-three levels (BBD) was used for the optimization of process parameters. The predicted value in the established model agreed well with the actual value. The chloride ion removal reached 68.7% with an operating cost of 10.68 \$/m^3 wastewater under the optimum conditions of the current density of 690 A/m^2, pH value of 8, and electrolysis time of 90 min.

Keywords: Wastewater; Chloride ion; Desulfurization; Coal-fired power plant

---

1. Introduction

Desulfurization wastewater is complex industrial wastewater generated from limestone–gypsum wet flue–gas desulfurization [1,2]. In the desulfurization progress, the chloride ion (Cl^-) will be enriched and become increasingly high. The concentration of chloride ions in some power plants could reach 10,000–20,000 mg/L. This ultra-high concentration of chloride ions reduces the effectiveness of desulfurization, affects the quality of the gypsum, and accelerates the equipment corrosion. Therefore, the removal of chlorides from desulfurization wastewater has become a practical problem and deserves in-depth study. Treatment of this type of wastewater is very difficult due to its high concentration of Cl^-. Besides, it is difficult to remove ultra-high concentration chloride ions (about 20,000 mg/L) in desulfurization wastewater by traditional methods [3]. In order to reuse the desulfurization wastewater, the concentration of chloride ions must be reduced by more than 50%, according to the requirement of a coal-fired power plant enterprise in Xinjiang province, China. In recent years, multi-effect evaporation crystallization is used to solve the crystallization of chlorides. However, this method consumes a lot of energy. The increased Cl^- concentration would corrode the materials used in the reactor and produce a new solid waste [4].

Therefore, the development of new processes for the efficient treatment of various industrial wastewaters with relatively low operating costs is urgent nowadays [5–8]. Recently, many investigations have pointed out that the use of advanced oxidation processes (AOPs) are desirable [9–11]. Especially, the electro-catalysis process has attracted

---

* Corresponding author.

1944-3994/1944-3986

great attention due to the easy operation, excellent effect, and no discharge of secondary pollution to the environment [12–15]. However, to the best of our knowledge, there is little literature that studied the optimization of the electro-catalysis progress using $Ti/SnO_2–Sb_2O_3/PbO_2$ electrode to treat the Cl^- from desulfurization wastewater. The mechanism of removing chloride ions was proposed as following: the electro-catalysis process based on the employment of $Ti/SnO_2–Sb_2O_3/PbO_2$ anode is presented in Eq. (1). A hydrogen evolution reaction occurs simultaneously at the cathode to form H_2 and OH^- through Eq. (3). There are some side reactions in the solution as shown in Eqs. (5)–(7) [16]. Under alkaline conditions, the side reactions produce ClO^- ions, which will be converted into Cl^- ions via Eq. (4) and finally be removed by the main reaction (Eq. (1)). The produced Cl_2 gas on the anode side was absorbed by an absorption tank.

On the anode side:

$$2Cl^- - 2e^- \rightarrow Cl_2\uparrow \quad (1)$$

$$4OH^- - 4e^- \rightarrow 2H_2O + O_2\uparrow \quad (2)$$

On the cathode side:

$$2H_2O + 2e^- \rightarrow H_2\uparrow + 2OH^- \quad (3)$$

$$ClO^- + 2H_2O + 2e^- \rightarrow 2OH^- + Cl^- \quad (4)$$

Side reaction in solutions:

$$Cl_2 + 2OH^- \rightarrow ClO^- + Cl^- + H_2O \quad (5)$$

$$Cl_2 + H_2O \rightarrow HClO + H^+ + Cl^- \quad (6)$$

$$HClO + H_2O \rightarrow H^+ + ClO^- \quad (7)$$

It is well-known that the operating parameters determine the performance of electro-catalysis progress by using $Ti/SnO_2–Sb_2O_3/PbO_2$ electrodes. A lot of studies on the optimization process focused on the one-factor-at-a-time approach, which is time-consuming and cannot obtain optimization results [17]. Many experimental design methodologies such as reaction kinetics [18–20], artificial neural networks (ANNs) [21,22], and factorial design [23] response surface methodology (RSM) [24,25] have been investigated to optimize and to predict the results of treatment processes. Among these methods, RSM is a useful method for optimizing a process by combining several independent variables and their interactions [17,26–28]. It is a powerful statistical-based technique to evaluate the simultaneous effects of several variables and obtain the optimum conditions for desirable responses. This procedure reduces the number of experimental trials and cost. According to the interaction effects between the studied factors, this methodology could determine the combination of levels in order to optimize the process [17,29,30]. However, RSM has still not been used for electro-catalysis progress to optimize chloride ion removal from desulfurization wastewater.

Hence, this study aims to evaluate electro-catalysis processes for the removal of chloride ions from desulfurization wastewater and optimize the operating parameters. A Box–Behnken experimental design (BBD) with three factors-three levels was employed to evaluate the effects of current density, electrolysis time, and initial pH on the chloride ion percentage removal efficiency. The interactive effect of process variables, the optimization of electro-catalysis process parameters, and the operating costs were also investigated.

2. Materials and methods

2.1. Desulfurization wastewater and chemicals

The desulfurization wastewater employed in this work was taken from the outlet of a coal-fired power plant in Xinjiang province, China. Its characteristics are shown in Table 1.

The pH value of solution was monitored by a portable pH meter (Metteler–Toledo Instruments Co., Ltd., Shanghai). All analytical methods were carried out in accordance with the Standard Methods of the APHA (APHA, 1998). Chemical oxygen demand (COD) was determined using a closed reflux spectrophotometric method based on the Standard Methods. $AgNO_3$ solution of 200 g/L concentration was employed to deposit the chloride ion to eliminate the chloride ion interferences on COD analysis. The method was as follows: take 20.0 mL water sample into 250 mL reflux conical flask, then add 10.00 mL standard solution of dichromate reagent (0.2500 mol/L) and several zeolite, then drop $AgNO_3$ solution until brick-red precipitation occurs. If the amount of silver nitrate solution exceeded 5.0 mL, dilute the water sample again. The chloride ion concentration was determined by titration with a standard $AgNO_3$ solution and K_2CrO_4 solution as a color developer.

2.2. Experimental method

As shown in Fig. 1, a cylinder organic glass reactor with volume of 2,000 mL was employed for electro-catalysis experiment. The electronic cell was equipped with an electrode array: a reticular Titanium plate (10 cm × 6 cm × 0.2 cm) with a thin coating of $Ti/SnO_2–Sb_2O_3/PbO_2$ as anode and a same dimension titanium plate as cathode. The distance between the two electrodes was kept at 1 cm. In each experiment, 1,500 mL of wastewater was placed in the reactor. After the reaction, and the samples

Table 1
Characteristics of desulfurization wastewater used in the experiments

Parameter	Average value
pH	8~9
COD (mg/L)	1,072 ± 100
Turbidity (NTU)	28 ± 5
Conductivity (mS/cm)	40.2 ± 10
Chloride (mg/L)	19,900 ± 200

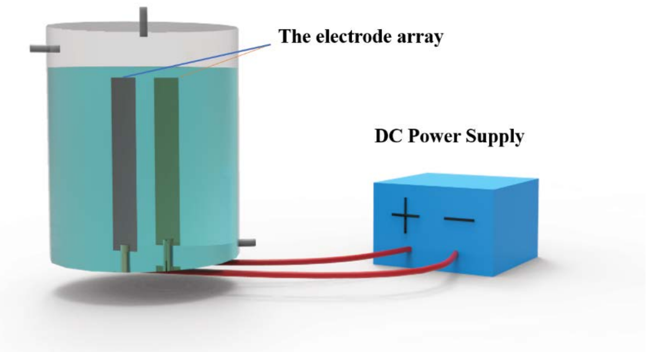

Fig. 1. Bench-scale electro-catalysis with electrode array in parallel connection.

were collected for further analysis. All experiments were performed at constant temperature (25°C). Every electro-catalysis experiment were carried out twice in parallel. The percentage removal efficiency of chloride ion was calculated using the following equation:

$$\text{Percentage removal efficiency}(\%) = \left(\frac{C_0 - C}{C_0}\right) \times 100 \tag{8}$$

where C_0 and C the initial and final concentrations of chloride ion.

2.3. BBD response surface design

To investigate the individual and interactive effects of process variables on the percentage of the chloride ion removal efficiency, a BBD based response surface method (RSM) with independent variables was employed. Based on our previous study [31] and the single factor experiment, the independent variables of current density (A), time (B), and pH value (C) were selected for modeling and optimization of the electro-catalysis process. Response surface method was adopted to optimize the conditions under the assumption of the influence of experimental factors on chloride ion removal rate was curvilinear. According to the response surface BBD principle, three factors including current density, time, pH after the test results were obtained, response surface analysis method with 3 factors and 3 levels was adopted to obtain the quadratic regression equation and find out the best process parameters. The levels of the variables used in the experiments were shown in Table 2. The Cl^- removal (%) was selected as the dependent response variable. The quadratic model was used to predict the relationship between independent variables and dependent response variables for the electro-catalysis progress as given in Eq. (9):

$$Y = a_0 + a_1x_1 + a_2x_2 + a_3x_3 + a_{11}x_1^2 + a_{22}x_2^2 + a_{33}x_3^2 + a_{12}x_1x_2 + a_{13}x_1x_4 + a_{23}x_2x_3 \tag{9}$$

where, Y is the response value (Cl^- removal efficiency, %); x_1, x_2, and x_3 represent the levels of the three independent variables (current density (A), time (B), and pH value (C)); a_0 is the intercept; a_1, a_2, and a_3 are the linear regression coefficients; a_{11}, a_{22}, and a_{33} represent the quadratic regression coefficients; a_{12}, a_{13}, and a_{23} are the interaction regression coefficients.

Table 2
Coded and actual values of the variables of the design of experiments for the overall electro-catalysis optimization

Factor	Independent variable	Range and level		
		–1	0	+1
A	Current density (A/m^2)	500	700	900
B	Time (min)	60	90	120
C	pH value	6	8	10

3. Results and discussion

3.1. ANOVA analysis

In order to check the statistical significance of the fitted quadratic models and analyze the results, the analysis of variances (ANOVA) was conducted by using the software Design Expert 11. The full factorial BBD with three factors in three levels and the results of Cl^- removal efficiency was illustrated in Table 3.

The data were fitted to the quadratic models and the significance and adequacy were tested by the ANOVA. As shown in Table 4, the overall ANOVA of the model shows that F is 350.948 and P is far less than 0.001, indicating that the model is valid and statistically significant. The ANOVA of the misfitting term shows that the F-value is 3.241 and P is greater than 0.05, indicating that the model is reasonable. There is no need to fit higher order equations and introduce more independent variables. The model determination coefficient was 0.997 and the adjustment determination coefficient was 0.995, indicating that 99.5% of the change in response value came from the selected factors. Coefficient of variation (CV%) was used to evaluate the degree of variation between different levels of the treatment group. The value of the adjusted determination coefficient (adjusted $R^2 = 0.994$) also proved the high significance of this model. The low value of the coefficient of variation (C.V. = 1.33%) suggested the reliability and the high precision of the experimental runs. The signal to noise ratio (adeq. precision) is usually expected to be greater than 4. In this model, the signal-to-noise ratio of the model is 47.08, which indicates the model could accurately reflect the experimental results.

The values of all regression coefficients with the selected levels are given in Table 5. As can be seen, B-time (min), C-pH, AB, AC, BC, A^2, B^2, and C^2 have significant effects on the removal rate of Cl^- as the P is less than 0.01, indicating that A, B, and C factors have linear and quadratic effects on the removal rate of chloride ions. Among these factors, it is concluded that the developed mathematical models have the ability to describe the electro-catalysis process. On the basis of the estimation of the coefficients (Table 5), the response functions with the determined coefficients for Cl^- removal are presented by the equation:

Table 3
Experimental design matrix and results of Cl^- removal efficiency

Run	*A*: current density (A/m^2)	*B*: time of electrolysis (min)	*C*: pH	Cl^- removal (%)
1	0	0	0	68.01
2	0	1	1	48.89
3	–1	0	1	58.35
4	–1	–1	0	42.12
5	0	–1	1	63.48
6	1	1	0	44.36
7	0	1	–1	62.98
8	0	0	0	68.54
9	1	–1	0	52.69
10	0	0	0	69.01
11	0	–1	–1	41.69
12	0	0	0	68.05
13	1	0	–1	54.31
14	–1	1	0	56.36
15	1	0	1	47.62
16	0	0	0	69.18
17	–1	0	–1	41.23

Table 4
ANOVA test for the quadratic models

Standard deviation	0.750767	*R*-squared	0.997789
Mean	56.28647	Adj. *R*-squared	0.994946
C.V. %	1.333832	Pred. *R*-squared	0.973923
PRESS	46.52749	Adeq. precision	47.08222

$$\text{Chloride ion removal (\%)} = 68.56 + 0.12A + 1.58B + 2.27C - 5.64AB - 5.95AC - 8.97BC - 11.78A^2 - 7.90B^2 - 6.40C^2 \quad (10)$$

3.2. Analysis of response surface

3.2.1. Overall effect analysis of the selected factors

The factors selected in this experiment have the quadratic effect, linear effect, and interaction effect on the removal rate of chloride ions. As shown in Fig. 2, response values appear to increase rapidly after a certain value and then began to decline with the increase of the factor level. It can be seen from the three factors of variations in the steep degree of wave pattern that current density (*A*) is higher than time (*B*), while time (*B*) is higher than pH

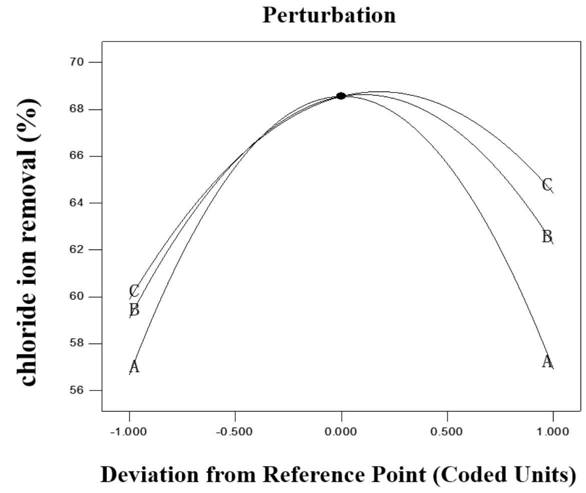

Fig. 2. Wave pattern of each factor.

Table 5
Estimated regression coefficients and corresponding significance level

Source	Sum of squares	df	Mean square	*F*	*P*	Saliency
Model	1,780.311	9	197.8123	350.9484	<0.0001	**
A: current density (A/m^2)	0.1058	1	0.1058	0.187705	0.6779	**
B: time (min)	19.87651	1	19.87651	35.26388	0.0006	**
C: pH	41.08711	1	41.08711	72.89463	<0.0001	**
AB	127.3512	1	127.3512	225.94	<0.0001	**
AC	141.729	1	141.729	251.4483	<0.0001	**
BC	321.8436	1	321.8436	570.9983	<0.0001	**
A^2	584.1888	1	584.1888	1,036.438	<0.0001	**
B^2	262.5462	1	262.5462	465.7958	<0.0001	**
C^2	172.544	1	172.544	306.1187	<0.0001	**
Residual	3.945555	7	0.563651			
Lack of fit	2.795675	3	0.931892	3.241701	0.1428	
Pure error	1.14988	4	0.28747			
Cor. total	1,784.256	16				

*$p < 0.05$ means significant, **$p < 0.01$ means extremely significant.

value (*C*). It can conclude that the current density and the electro-catalysis time determine the Cl⁻ removal efficiency. As the concentration of chloride ions must be reduced by more than 50% to meet the requirement of the enterprise in Xinjiang province, China. The optimum current density and time need to be properly selected.

3.2.2. Interaction analysis among different factors

Response surface analysis diagram is an 3D surface diagram composed of response values and each variable, showing the influence of the other two factors on the removal rate of chloride ion. The higher the slope of response surface diagram, the greater the influence of this factor on chloride ion removal rate. However, when two factors interact, the influence process of one factor on chloride ion removal rate is different at different levels. The contour map is on the surface of the same response values to form in the bottom curve. When the contour tends to be more rounds, it shows that the interaction of the two is smaller. If the contour lines in the ellipse are closer, it indicates that the interaction of the two is bigger. The intensity of contour reflects the degree of the influence of factors on the chloride ion removal rate. The more intense contour means the greater effect on chloride ion removal rate.

It can be seen from Fig. 3a that the contour line of current density (*A*) and time (*B*) factors present an ellipse from the upper left to the lower right, indicating that current density (*A*) and time (*B*) factors interact. As the contour density of *A* factor is higher than that time (*B* factor), exhibiting that current density (*A*) has a higher influence on Cl⁻ removal rate than time (*B*). The current density is one of the effective parameters in the electrochemical process, which influences the process efficiency significantly. For this purpose, the current density in the range of 500–900 A/m² was investigated for the chloride ion removal rate. As shown in Fig. 3b, chloride ion removal rate also increases with the increase of current density. Because the formation of Cl_2 rate is mainly controlled by the applied current density during electrolysis. The chloride ion removal rate began to fall when the current density is more than a certain value (680–710 A/m²). The results showed that the highest chloride ion removal efficiency was obtained at higher current densities, which is in good agreement with the results of the present study [31]. Because of the interaction effect, under the different level of time (*B*) factors, the level of current density factor increases on chloride ion removal rate changes have differences. Chloride ion removal rate decline slowly and then increasing rapidly when time factor is at low level with the increase of factor. Under the high level of the time factor, with the increase of current density factor, chloride ion removal declines faster after slowly rising. With the increase of time factor, the chloride ion removal rate also increases. When the time is more than a certain value (85–98 min), the chloride ion rate begins to fall. Because of the interaction, under different levels of current density factor, the increase of time factors leads to chloride ion removal rate changes have the difference. When the current density is low, with the increase of time, chloride ion removal rate slowly declined after increasing rapidly. When factor current density factor is high level, with the increase of operating time, chloride ion removal rate declined rapidly after rising slowly. This phenomenon agrees well with many previous electro-catalysis study [32].

As shown in Fig. 4a, the contour line of current density (*A*) and pH (*C*) factors present an ellipse from the upper left to the lower right, indicating that there is an interaction between *A* and *C* factors. The density of the contour line of factor *A* is higher than that of *C* factor, which suggests that the current density factor has a higher influence on the chloride ion removal rate than the pH factor. In the electro-catalysis progress, the initial pH has also been observed to be a very important factor. In order to evaluate this parameter, the experiments were carried out at different initial pH values (6–10). As shown in Fig. 4b, with the increase

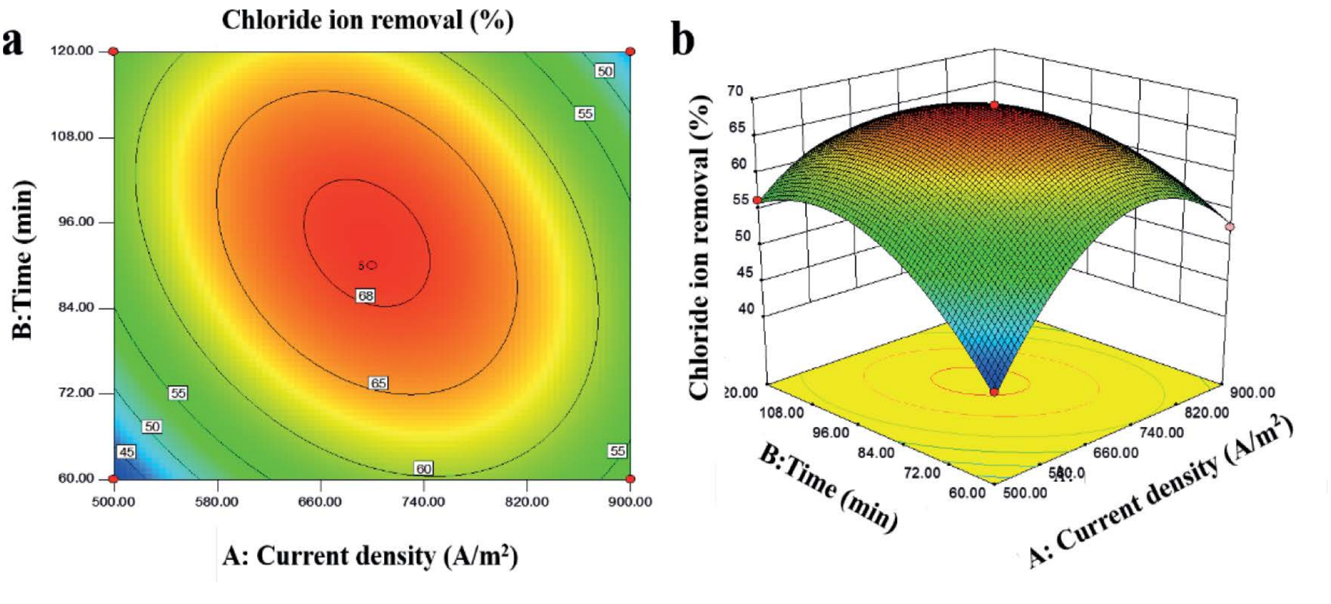

Fig. 3. (a and b) Interaction of the factors current density (*A*) and the time (*B*).

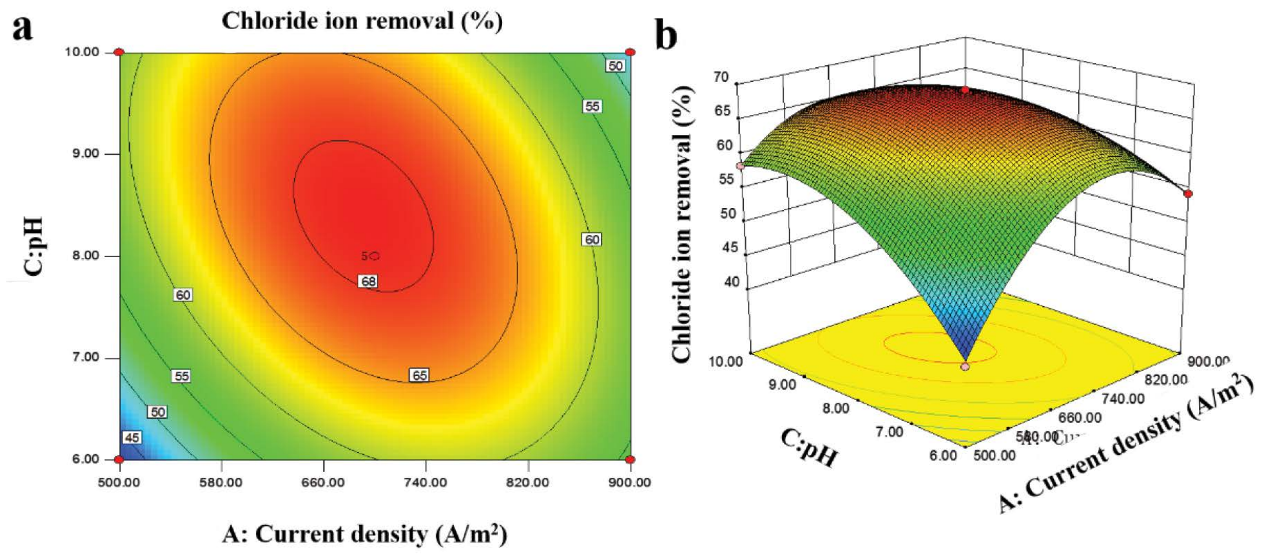

Fig. 4. (a and b) Interaction of factors current density (*A*) and pH (*C*).

of current density (*A*) levels, the chloride ion removal rate increases. When the current density is more than a certain value (670–710 A/m^2), the chloride ion removal rate began to fall. Because of the interaction, when the pH factor was low, with the increase of current density, the chloride ion removal rate increased quickly after a slow drop. When the pH factor was high level, the chloride ion removal slow declined after rising slowly with the increase of current density. With the increase of pH factors the chloride ion removal rate also raised. After a certain value (7.5–9.0), the chloride ion removal rate began to fall. But the change was very slight. Base on the previous study [31], the porous Ti/SnO_2–Sb_2O_3/PbO_2 electrode has a good removal effect over the whole range of pH values. Because of the interaction, when the current density is at a low level, with the increase of pH, the chloride ion removal rate slow declined after increasing rapidly. When the current density was at a high level, with the increase of pH, the chloride ion removal rate declined rapidly after slowly rising. This may be attributed to the interaction between current density and pH values.

As shown in Fig. 5a, the contour line of operating time (*B*) and initial pH (*C*) factors presents an ellipse from the upper left to the lower right. The contour density of *B* factors is higher than that of *C* factor. It indicated that *B* factors have a higher influence on chloride ion removal rate than *C* factors. Increasing electrolysis time in many progresses could lead to greater contact between the electrode and the pollutant and increased removal efficiency. To study the effect of electrolysis time on the removal of chloride ions, electrolysis time was selected in the range of 60–120 min.

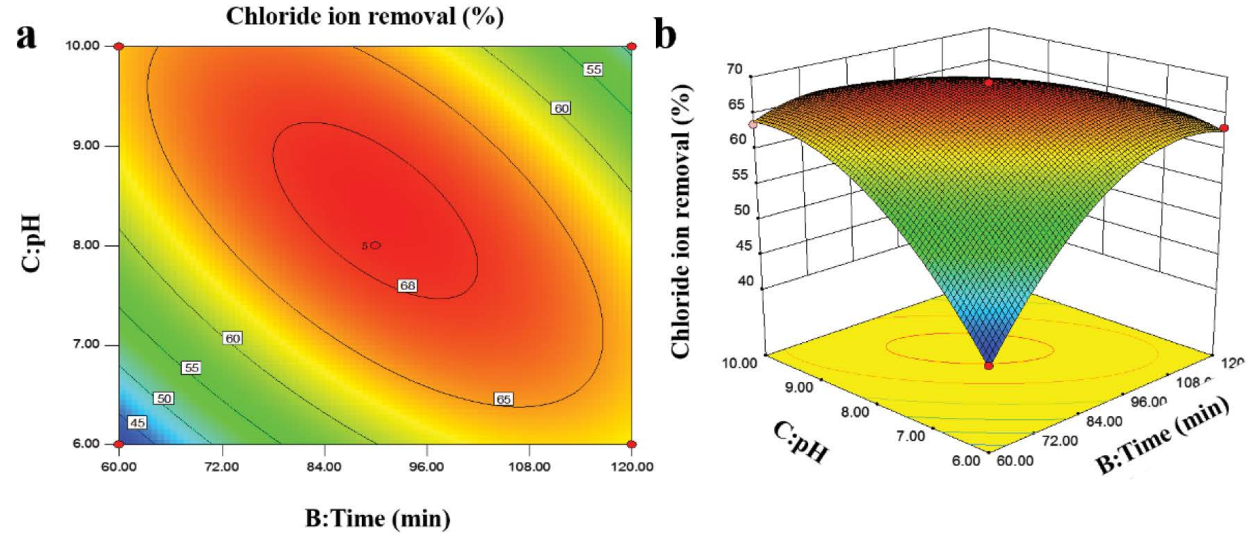

Fig. 5. (a and b) Interaction of factors current density (*A*) and pH (*C*).

The results showed that electrolysis time was directly correlated with the chloride ion efficiency. It can be seen from Fig. 5b that the chloride ion removal rate increases with the increase of time. When the operating time was higher than a certain value (84–100 min), the chloride ion removal rate began to fall. Because of the interaction, when pH factor was low, with the increase of time, the chloride ion removal rate increased quickly after a slow drop. The chloride ion removal rate declined rapidly after a slow rise with the increase of operating time when pH was at a high level. The chloride ion removal rate rises with the increase of pH factors. When the pH value was more than 7.5–9.0, the chloride ion removal rate began to fall. Because of the existence of interaction at different levels in operating time, when the time was low, with the increase of pH factors, the chloride ion removal rate slowly declined after a faster increase. When the operating time was at a high level, along with the increase of the pH factor levels, the chloride ion removal rate rises slowly and then decline rapidly. The results showed that electrolysis time was directly correlated with chloride ion so that it was increased by increasing electrolysis time from 60 to 120 min. The obtained results indicate that the chloride ion removal was increased rapidly with increasing operating time at the early reaction, but kept smooth growth after 60 min [31].

3.3. Optimization of electro-catalysis process parameters and validation of the models

The suitability of the mathematical model equations for predicting the optimum response values were tested using the selected optimal conditions. The result showed that the optimized conditions were the current density of 690.88 A/m², the time of 90.17 min, and the pH of 8.39. Under these conditions, the theoretically predicted value of the removal rate of chloride ions was 68.78%. Under the optimal theoretical conditions, three experiments were conducted when the current density of 691 A/m², the time of 90 min, and the pH 8.4, the results were 68.75% ± 3.245%, which was very close to the predicted value in theory and the error was less than 5%. It is indicated that the optimal process conditions were reasonable and feasible. As shown in Fig. 6, the residuals normal diagram also indicates that residuals are closely distributed around the diagonal line, which satisfies the normality.

A series of experiments were conducted to verify the model. The scatter points of both the actual and predicted values were given in Fig. 7. It can be seen that the predicted vs. experimental plot for the Cl^- removal were distributed near to the straight line. The scatter points are closely distributed around the diagonal, which indicates the predicted values and the actual values fit well. Thus, it was a suitable model to predict chloride ion removal efficiency. According to the established model, the predicted value was very close to the experimental data.

3.4. Operating costs of the electro-catalysis process for the chloride ion removal

The operating costs (OC) of the electro-catalysis process for the chloride ion removal were calculated by combining the electrodes cost, the electrical energy cost, chemicals, as well as labor, maintenance costs [33]. In this electro-catalysis process, the energy, electrode material were taken into account as major cost items in the calculation of the OC as \$/m³ for the removal of chloride ion wastewater [34,35]:

$$\mathrm{OC} = xC_{\mathrm{energy}} + yC_{\mathrm{electrode}} \tag{11}$$

where the constants x, y were provided by the China market in September 2019 with a value of electrical energy price (0.1 \$ /kWh), electrode price (40 \$/m²), respectively.

Specific energy consumption per volume of treated model wastewater (kWh/m³) can be calculated by the following equation [36]:

$$C_{\mathrm{energy}} = \frac{I \times V \times t}{V_{\mathrm{waster\ water}}} \tag{12}$$

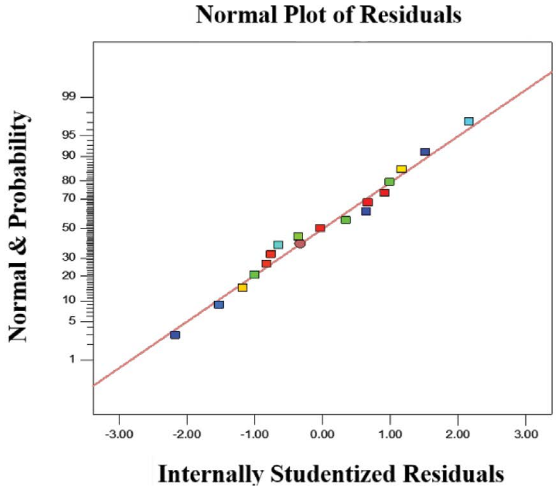

Fig. 6. Residuals normal diagram.

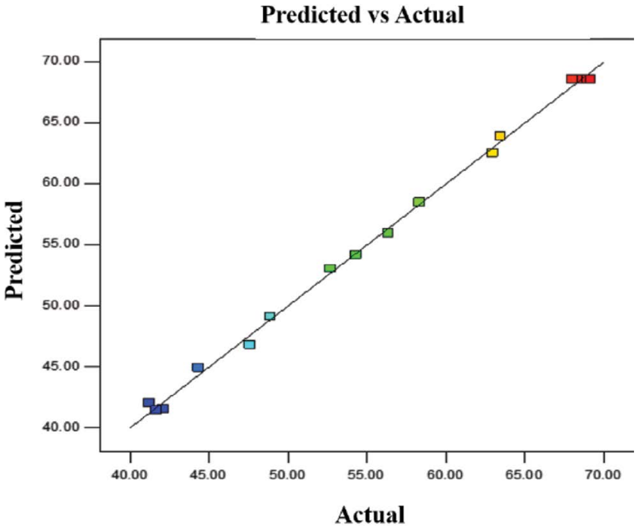

Fig. 7. Predicted vs. experimental data regarding the Cl^- removal efficiency.

where I is the applied current (A), V is the voltage (V), t is the operation time (h), and V is the volume of the desulfurization wastewater (m^3). It was found that when 690 A/m^2 current density was applied, energy consumption was 82.8 kWh/m^3. According to the equations, OC for the electro-catalysis process for 68% removal of chloride ion was calculated as 10.68 \$/m^3, which was an acceptable price for the power enterprises. Compared with other work in the electrolysis–electrodialysis process for removing chloride ions [37], Cui et al. use pure Ti and Ti-based ruthenium–iridium–titanium coatings as the anode and cathode materials. Under the optimal condition, the treatment cost from the energy consumption is 0.15 \$/kg Cl^-, with considering the profit of the Cl_2, H_2, and $Ca(OH)_2$ by-products. Especially, the electro-catalysis process required no feeding device which is economically feasible, industrially feasible, and worth popularizing.

4. Conclusion

In order to effectively remove ultra-high concentration chloride ions in desulfurization wastewater, the performance of electro-catalysis progress for chloride ion removal from desulfurization wastewater was investigated in a laboratory-batch study. The experimental parameters were optimized by using an RSM with BBD. Three factors-three levels Box–Behnken response surface design was used for the optimization of the process including current density, electrolysis time, and pH value. Their interactive effects on the response of chloride ions removal were also studied. The optimal process parameters were that the current density was 690 A/m^2, the time was 90 min, and the pH was 8. With the effect of $Ti/SnO_2–Sb_2O_3/PbO_2$ electrodes, the concentration of chloride ions can be removed by more than 50%. A reduction in the concentration of chloride ions can reduce the corrosion of equipment. Under these conditions, the removal rate of chloride ions was 68.78 %, and the operating cost was 10.68 \$/m^3 wastewater. The results indicated that a BBD can be applied to identify the most significant operating parameter for removing a chloride ion from desulfurization wastewater during an electro-catalysis reaction. It can provide guidance for the potential industrial application.

Acknowledgments

The authors gratefully acknowledge financial support from the National Natural Science Foundation of China (No. 51876162).

References

[1] Z. Sun, S. Wang, Q. Zhou, S.e. Hui, Experimental study on desulfurization efficiency and gas–liquid mass transfer in a new liquid-screen desulfurization system, Appl. Energy, 87 (2010) 1505–1512.

[2] L. Zhou, Y. Liu, L.Y. Luo, Z.L. Yuan, L.J. Yang, H. Wu, Improving the removal of fine particles by chemical agglomeration during the limestone-gypsum wet flue gas desulfurization process, J. Environ. Sci. China, 80 (2019) 35–44.

[3] S.W. Pan, N. Tang, J.J. Hu, J.F. Kuang, M. Qi, K. Ye, Experimental study on the spray of mercury removal performance of flue gas desulfurization wastewater, Adv. Mater. Res., 807–809 (2013) 1483–1488.

[4] G. Riedel, C. Voigt, H. Werner, U. Heubner, Qualification of metallic materials for evaporation of waste water from flue gas desulfurization plants, Mater. Corros., 50 (1999) 452–462.

[5] R.C. Peng, P. Yu, Y.B. Luo, Coke plant wastewater posttreatment by Fenton and electro-Fenton processes, Environ. Eng. Sci., 34 (2017) 89–95.

[6] R.C. Peng, H.L. Zhang, L. Gui, Z.K. Wu, P. Yu, Y.B. Luo, Facile synthesis of MnO_2@cellulose composite film, Environ. Eng. Sci., 36 (2019) 583–588.

[7] C.C. Dong, J.H. Ji, B. Shen, M.Y. Xing, J.L. Zhang, Enhancement of H_2O_2 decomposition by the co-catalytic effect of WS2 on the Fenton reaction for the synchronous reduction of Cr(VI) and remediation of phenol, Environ. Sci. Technol., 52 (2018) 11297–11308.

[8] M. Ahmaruzzaman, V.K. Gupta, Rice husk and its ash as low-cost adsorbents in water and wastewater treatment, Ind. Eng. Chem. Res., 50 (2011) 13589–13613.

[9] J.S. Chen, J.D. Zhang, Y.Z. Xian, X.Y. Ying, M.C. Liu, L.T. Jin, Preparation and application of TiO_2 photocatalytic sensor for chemical oxygen demand determination in water research, Water Res., 39 (2005) 1340–1346.

[10] L. Gui, J.H. Peng, P. Li, R.C. Peng, P. Yu, Y.B. Luo, Electrochemical degradation of dye on TiO_2 nanotube array constructed anode, Chemosphere, 235 (2019) 1189–1196.

[11] A. Shokri, The treatment of spent caustic in the wastewater of olefin units by ozonation followed by electrocoagulation process, Desal. Water Treat., 111 (2018) 173–182.

[12] L. Gui, H.Y. Jin, Y. Zheng, R.C. Peng, Y.B. Luo, P. Yu, Electrochemical degradation of bisphenol A using different modified anodes based on titanium in aqueous solution, Int. J. Electrochem. Sci., 13 (2018) 7141–7156.

[13] K. Chiang, T.M. Lim, L. Tsen, C.C. Lee, Photocatalytic degradation and mineralization of bisphenol A by TiO_2 and platinized TiO_2, Appl. Catal., A, 261 (2004) 225–237.

[14] L. Ciriaco, C. Anjo, M.J. Pacheco, A. Lopes, J. Correia, Electrochemical degradation of Ibuprofen on $Ti/Pt/PbO_2$ and Si/BDD electrodes, Electrochim. Acta, 54 (2009) 1464–1472.

[15] Y.H. Cui, X.Y. Li, G.H. Chen, Electrochemical degradation of bisphenol A on different anodes, Water Res., 43 (2009) 1968–1976.

[16] S. Neodo, D. Rosestolato, S. Ferro, A. De Battisti, On the electrolysis of dilute chloride solutions: influence of the electrode material on Faradaic efficiency for active chlorine, chlorate and perchlorate, Electrochim. Acta, 80 (2012) 282–291.

[17] H. Xu, M. Li, F.M. Wu, J. Zhang, Optimization of Fenton oxidation process for treatment of hexogeon industrial wastewater using response surface methodology, Desal. Water Treat., 55 (2015) 77–85.

[18] A.T. Marshall, A. Herritsch, Understanding how the oxygen evolution reaction kinetics influences electrochemical wastewater oxidation, Electrochim. Acta, 282 (2018) 448–458.

[19] X.Q. Yin, B. Jing, W.J. Chen, J. Zhang, Q. Liu, W. Chen, Study on COD removal mechanism and reaction kinetics of oilfield wastewater, Water Sci. Technol., 76 (2017) 2655–2663.

[20] A. Shokri, A kinetic study and application of electro-Fenton process for the remediation of aqueous environment containing toluene in a batch reactor, Russ. J. Appl. Chem., 90 (2017) 452–457.

[21] F.H. Kamar, F.E. Niamat, A.A.H. Faisal, A.A. Mohammed, A.C. Nechifor, G. Nechifor, Use of artificial neural network for modeling and prediction of reactive red dye removal from wastewater using banana peels bio-sorbent, Rev. Chim., 69 (2018) 1919–1926.

[22] F. Schmitt, R. Banu, I.T. Yeom, K.U. Do, Development of artificial neural networks to predict membrane fouling in an anoxic-aerobic membrane bioreactor treating domestic wastewater, Biochem. Eng. J., 133 (2018) 47–58.

[23] A. Shokri, Application of sono–photo-Fenton process for degradation of phenol derivatives in petrochemical wastewater using full factorial design of experiment, Int. J. Ind. Chem., 9 (2018) 295–303.

[24] C.O. Guimaraes, A.B. Franca, G.R.L. Samanamud, E.P. Baston, R.C.Z. Lofrano, C.C.A. Loures, L.L.R. Naves, F.L. Naves, Optimization of treating phenol from wastewater through the TiO_2-catalyzed advanced oxidation process and response surface methodology, Environ. Monit. Assess., 191 (2019) 349–362.

[25] Z. Ghasemi, H. Younesi, A.A. Zinatizadeh, Preparation, characterization and photocatalytic application of TiO_2/Fe-ZSM-5 nanocomposite for the treatment of petroleum refinery wastewater: optimization of process parameters by response surface methodology, Chemosphere, 159 (2016) 552–564.

[26] X. Zhu, J. Tian, R. Liu, L. Chen, Optimization of Fenton and electro-Fenton oxidation of biologically treated coking wastewater using response surface methodology, Sep. Purif. Technol., 81 (2011) 444–450.

[27] E.E. Mitsika, C. Christophoridis, K. Fytianos, Fenton and Fenton-like oxidation of pesticide acetamiprid in water samples: kinetic study of the degradation and optimization using response surface methodology, Chemosphere, 93 (2013) 1818–1825.

[28] A. Shokri, Employing electrocoagulation for the removal of Acid Red 182 in aqueous environment by using Box–Behenken design method, Desal. Water Treat., 115 (2018) 281–287.

[29] S.M.B. Hosseini, N. Fallah, S.J. Royaee, Optimization of photocatalytic degradation of real textile dye house wastewater by response surface methodology, Water Sci. Technol., 74 (2016) 1999–2009.

[30] W.Z. Jiao, L.S. Yu, Z.R. Feng, L. Guo, Y.H. Wang, Y.Z. Liu, Optimization of nitrobenzene wastewater treatment with O_3/H_2O_2 in a rotating packed bed using response surface methodology, Desal. Water Treat., 57 (2016) 19996–20004.

[31] K.D. Xu, J.H. Peng, P. Chen, W.K. Gu, Y.B. Luo, P. Yu, Preparation and characterization of porous Ti/SnO_2-Sb_2O_3/PbO_2 electrodes for the removal of chloride ions in water, Processes, 7 (2019) 762–776.

[32] K. Thirugnanasambandham, V. Sivakumar, Optimization of treatment of grey wastewater using electro-Fenton technique – modeling and validation, Process Saf. Environ. Prot., 95 (2015) 60–68.

[33] R.C. Peng, P. Yu, Y.B. Luo, A comparative study of Fenton and electro-Fenton treatment for COD removal from coking industry wastewater, Fresenius Environ. Bull., 25 (2016) 3987–3992.

[34] M. Kobya, S. Delipinar, Treatment of the baker's yeast wastewater by electrocoagulation, J. Hazard. Mater., 154 (2008) 1133–1140.

[35] A. Akyol, O.T. Can, E. Demirbas, M. Kobya, A comparative study of electrocoagulation and electro-Fenton for treatment of wastewater from liquid organic fertilizer plant, Sep. Purif. Technol., 112 (2013) 11–19.

[36] J. Virkutyte, E. Rokhina, V. Jegatheesan, Optimisation of electro-Fenton denitrification of a model wastewater using a response surface methodology, Bioresour. Technol., 101 (2010) 1440–1446.

[37] L. Cui, G. Li, Y. Li, B. Yang, L. Zhang, Y. Dong, C. Ma, Electrolysis-electrodialysis process for removing chloride ion in wet flue gas desulfurization wastewater (DW): influencing factors and energy consumption analysis, Chem. Eng. Res. Des., 123 (2017) 240–247.